Laser-Driven Shock Waves in an Aerosol-Induced Breakdown in Air

P. Vigliano,* M. Autric,† J. P. Caressa,‡ V. Chhim,§ and D. Dufresne¶
Institute of Fluid Mechanics, Marseille, France

Aerosol-induced breakdown strongly limits the propagation of high-power laser pulses through the atmosphere. Indeed, when air breaks down due to an intense laser pulse, the high-pressure, high-density plasma generated is highly absorbing to the incident laser radiation. Plasma expands, fills the laser beam, and subsequently blocks off the laser energy. The purpose of this paper is to present a simple hydrodynamical model to simulate the development of the plasma resulting from the breakdown initiated by the aerosols hanging in the air. This model describes the expansion of an unsteady spherical shock wave. Experimental investigations (time-integrated, framing, streak, and schlieren photographs recording the plasma luminosity and shock wave) have been conducted to evaluate the accuracy of the model.

Nomenclature

A,B,C,D = constants in shock motion [Eq. (5)]
c = speed of light
c_0 = reference sound speed
E = laser energy per pulse
e = charge of the electron
G = rate of energy addition
g = Gaunt's factor
h = Planck's constant
I = energy integral in dimensionless equations
K_ν = inverse bremsstrahlung absorption coefficient
k = Boltzmann's constant
M = Mach number
m = mass of the electron
N_e = electronic density
N_+ = ionic density
p = gas pressure
$\tilde{p}$ = dimensionless gas pressure
$R(t)$ = shock wave position
R_0 = dimensionless explosion length
r = spherical radius
r_s = dimensionless shock wave position
T = plasma temperature
T_c = time of breakdown
t = time
u = gas velocity
$\tilde{u}$ = dimensionless gas velocity
V = shock wave velocity
V_A, V_R = axial and radial velocity, respectively
X_A, X_R = axial and radial development, respectively
α = power in the power law density
α_1,α_2,β = constants in laser pulse formula [Eq. (8)]
γ = ratio of specific heats
η = shock strength parameter
θ = shock decay coefficient
ν = laser frequency
ξ = dimensionless spherical radius
ρ = gas density
ρ_0 = density of the ambient air
$\tilde{\rho}$ = dimensionless gas density
τ = dimensionless time
ϕ = laser intensity
$\tilde{\phi}$ = average laser intensity
ϕ_a = laser intensity absorbed by the plasma
ϕ_{peak} = maximum laser intensity

Received April 13, 1983; revision received Dec. 22, 1983.

*Research Scientist, Université de Toulon et du Var; also working with the Institute of Fluid Mechanics.
†Research Scientist, Centre National de la Recherche Scientifique. Member AIAA.
‡Research Scientist, Centre National de la Recherche Scientifique.
§Maître-Assistant, Université Aix-Marseille II.
¶Maître-Assistant, Université Aix-Marseille II. Member AIAA.

Introduction

NUMEROUS previously published experimental and theoretical investigations[1-11] on the aerosol-induced breakdown and the dynamics of laser-induced plasmas have been conducted for 1.06 μm (Nd), 2.7 μm (HF), 3.8 μm (DF), and 10.6 μm (CO_2) wavelengths. When the laser intensity and fluence are high enough to cause breakdown of the aerosol particles naturally suspended in the air, the plasma created around each particle absorbs the incident laser radiation according to the inverse bremsstrahlung absorption process and subsequently expands axially and radially. This phenomenon leads to laser beam blockage. It is of interest for the propagation of a high-energy pulsed laser beam through the atmosphere to determine the development of the air plasma.

A computed numerical simulation of the propagation of laser beams through the atmosphere under these conditions has been worked out. In this simulation, a hydrodynamic model of the development of the plasma created around each particle is used. Three hydrodynamic models of the development of a sustained laser-driven shock wave previously worked out by different authors have been studied and their results have been compared[12]:

1) A laser-supported detonation wave model described by Raizer[13] in the case of a steady-state one-dimensional plane shock wave.

2) A laser-supported absorption wave model described by Edwards and Fleck.[14] This model uses optical considerations coupled with a three-temperature nonequilibrium thermodynamic model of the air plasma and two-dimensional Lagrangian hydrodynamics.

3) An unsteady spherical wave model related by Boni and Su.[15]

The purpose of this paper is to describe this last model, to present our obtained results, and to compare them with experimental data.

Unsteady Spherical Shock Wave Model

According to the theory of Bach and Lee,[16] which has given accurate results for the entire regime of blast wave propagation, a model describing the maintenance of laser-

driven shock waves in the unsteady spherical case may be developed from classical conservation equations of fluid mechanics:

Mass conservation

$$\frac{\partial \rho}{\partial t}+u\frac{\partial \rho}{\partial r}+\rho\frac{\partial u}{\partial r}+2\frac{\rho u}{r}=0 \tag{1}$$

Momentum conservation

$$\frac{\partial u}{\partial t}+u\frac{\partial u}{\partial r}+\frac{1}{\rho}\frac{\partial p}{\partial r}=0 \tag{2}$$

Energy conservation under the integral form

$$\pi R^2\phi_a(t)=4\pi\frac{\mathrm{d}}{\mathrm{d}t}\left\{\int_0^R\left(\frac{p}{\gamma-1}+\frac{\rho u^2}{2}\right)r^2\mathrm{d}r-\int_0^R\frac{p_0}{\gamma-1}r^2\mathrm{d}r\right\} \tag{3}$$

In accordance with Bach and Lee, a power law density is assumed

$$\tilde{\rho}(\xi,r_s)=\tilde{\rho}(1,r_s)\xi^{\alpha}$$

with the following dimensionless variables

$$\xi=\frac{r}{R(t)};\quad r_s=\frac{R(t)}{R_0};\quad \tilde{\rho}(\xi,r_s)=\frac{\rho(r,t)}{\rho_0}$$

α is determined by the mass conservation integral written in dimensionless form

$$\int_0^1\tilde{\rho}(\xi,r_s)\xi^2\mathrm{d}\xi=\tfrac{1}{3}$$

that implies

$$\alpha=3(\tilde{\rho}(1,r_s)-1)$$

It can be shown[15] that Eqs. (1-3) can be reduced to nonlinear ordinary differential equations as

$$\frac{\mathrm{d}I}{\mathrm{d}y}=-\frac{I}{y}\left(1+\frac{2\theta}{3}\right)+\frac{2\eta}{3\gamma(\gamma-1)y}+\frac{2}{3}G\frac{\eta^{3/2}}{y} \tag{4}$$

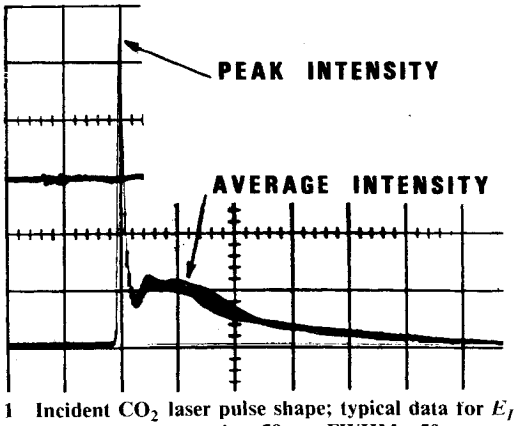

Fig. 1 Incident CO_2 laser pulse shape; typical data for $E_l=160$ J; $\tau_{pulse}=2.5$ μs; ramping portion 50 ns; FWHM=50 ns; peak power 0.5×10^9 W; ratio of peak power to tail power=5; ratio of spike energy to total energy=0.2; 500 ns/div.

$$\frac{\mathrm{d}\theta}{\mathrm{d}y}=-\frac{2\eta[1-A-B\theta-C\theta^2]}{3Dy} \tag{5}$$

$$\frac{\mathrm{d}\eta}{\mathrm{d}y}=-\frac{2\eta\theta}{3y} \tag{6}$$

$$\frac{\mathrm{d}\tau}{\mathrm{d}y}=\frac{\eta^{1/2}y^{-1/3}}{3} \tag{7}$$

with

$$I=\int_0^1\left|\frac{\tilde{p}}{\gamma-1}+\frac{\tilde{\rho}\tilde{u}^2}{2}\right|\xi^2\mathrm{d}\xi$$

$$\theta=\frac{R\ddot{R}}{\dot{R}^2},\qquad \eta=C_0^2/\dot{R}^2$$

$$G=(1-\exp(-K_\nu r),\frac{\phi_{\text{peak}}}{8\rho_0c_0^3}\left(\frac{1}{\cosh\alpha_1(t-t_1)}+\frac{\beta}{\cosh\alpha_2(t-t_2)}\right)$$

$$y=r_s^3,\qquad \tau=\frac{tc_0}{R_0}$$

$$K_\nu=\frac{4}{3}\left(\frac{2\pi}{3kT}\right)^{1/2}g\frac{Z^2e^6}{hcm^{3/2}\nu^3}N_+N_e(1-e^{-h\nu/kT})\ (\mathrm{cm}^{-1}) \tag{8}$$

where K_ν is the inverse bremsstrahlung absorption coefficient.[17]

A limited development of I, θ, y, and τ is used in the neighborhood of $\eta=0$. Then, the system of equations is numerically integrated by a fourth-order Runge-Kutta formula. We use the formula

$$t=\frac{R_0\tau}{c_0}\quad\text{and}\quad r(t)=\left(\frac{E_0}{4\pi\rho_0c_0^2}y\right)^{1/3}$$

to obtain trajectories of shock waves.

Numerical Results

Figure 1 shows the shape of the typical gain-switched laser pulse used in our experiments, modeled by the formula

$$\phi(t)=\phi_{\text{peak}}\frac{\cosh\alpha_2(t_1-t_2)}{\beta}\left(\frac{1}{\cosh\alpha_1(t-t_1)}+\frac{\beta}{\cosh\alpha_2(t-t_2)}\right)$$

with $t_1=0.05$ μs, $t_2=0.5$ μs, $\alpha_1=80$ μs^{-1}, $\alpha_2=2$ μs^{-1}, and $\beta=0.25$.

Figure 2 represents the velocities of the laser-driven shock waves as a function of time. The different curves are representative of various quantities of energy addition. The relative maxima of the velocity observed in Fig. 2 near 0.1 μs reflect the influence of the laser spike intensity. The level of the maximum is strongly dependent on the pulse energy. A delay time exists between the peak intensity and the relative maximum observed in the velocity curves. One can observe that this delay time decreases with an increase of laser energy.

Figure 3 shows the radial velocities of shock waves as a function of average and peak intensities. The values are those obtained during a 0.5 μs interval during which the laser intensity is relatively constant.

It is possible to compare in this figure the values of the radial expansion velocity for the previously presented hydrodynamic models.[12-19] The solid curve represents the velocity of a one-dimensional plane laser-supported detonation wave deduced from Raizer's theory ($V_R=\frac{1}{2}V_A$, $V_A=\frac{1}{2}[2(\gamma^2-1)(\phi/\rho_0)]^{1/3}$. The discontinuous curve represents the velocity deduced from Edwards' results over the intensity range extending from 10^7 to 10^8 W/cm^2 ($V_R=0.73V_A$). In this case,

the shock development differs from that of a one-dimensional laser-supported detonation wave due to its two-dimensional character. The dashed curve indicates the results of the present model ($V_R = V_A$). We can notice that, for an average intensity of 10^8 W/cm^2 (peak intensity 5×10^8 W/cm^2), the difference is about 30%.

Also, results of the plasma expansion velocity over the intensity range extending from 10^6 to 3×10^7 W/cm^2 published by Wu et al.[19] are plotted. Calculations have been made for the initial air plasma size $R_i = 0.05$ cm.

As can be observed from Fig. 3, the velocity is proportional to ϕ^1 over the intensity range extending from 10^6 to 3×10^7 W/cm^2. As the intensity increases to above 3×10^7 W/cm^2, the air plasma expansion is dominated by LSD wave propagation (proportional to $\phi^{1/3}$).

Experimental Investigations

At the same time, experimental investigations have been carried out to visualize and determine the development of the shock wave and luminous plasma created around each aerosol particle.

A scheme of the experimental setup is shown in Fig. 4. The following experiments have been performed with a cold-cathode electron-gun CO_2 laser which is used with an unstable optical resonator. It products an annular laser beam with a major diameter of about 10 cm and a minor diameter of about 6.6 cm. The beam has a full-angle beam divergence better than 8×10^{-4}rad. The laser is capable of producing up to 200 J with a pulse duration of 2.5 μs. The pulse used for air breakdown experiments consists of a high-power peak (typically 5×10^8 W/cm^2) with a full width at half-maximum duration of 50 ns followed by a lower powered tail which gives a constant flux during 0.5 μs. The ratio of energy between the peak and the tail is 0.2. As shown in Fig. 4, a small part of the beam is reflected by W_1 for monitoring by detectors (photon-drag detector and calorimeter). The temporal shape of the output pulse does not change significantly. The shot-to-shot energy variation is better than 10%.

The beam, focused with an appropriate mirror (5 m for this case), gives an annular intensity distribution with a central peak in the focal position. In this paper, the intensity is specified in terms of average intensity.

The time history of the created plasma ($t \leq 4$ μs) is recorded on a TRW streak camera, the slit of which is parallel to the laser beam axis and on an Imacon (image converter) camera (20×10^6 images/s). A typical streak photograph is shown in Fig. 5a for an average laser intensity of about 10^8 W/cm^2 (peak intensity 5×10^8 W/cm^2) in the focal region.

Schlieren records taken at different times after the onset of the breakdown show the axial and radial development of the shock waves surrounding the aerosol. Figure 5b presents a set of schlieren photographs, the first of which has been taken 4 μs after the initiation of the breakdown.

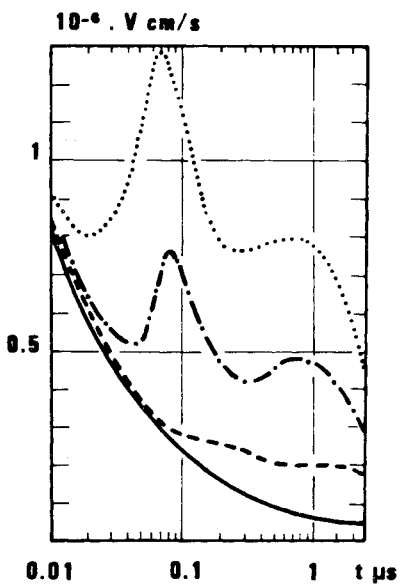

Fig. 2 Velocities of the laser-driven shock waves as a function of time for various average intensities: ·····, 10^9 W/cm^2; —·—·—, 10^8 W/cm^2; --------, 2×10^7 W/cm^2; and ————, velocity of a blast wave.

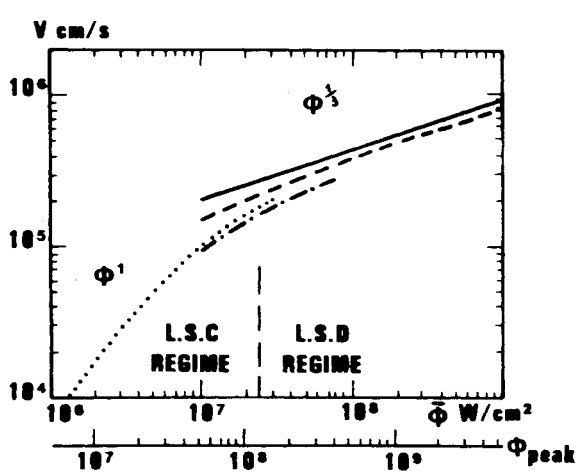

Fig. 3 Radial velocities of a laser-driven shock waves as a function of average and peak intensities deduced from different models. In the laser supported combustion regime: ··· Wu's model. In the LSD regime: —, one-dimensional LSD wave model: —·—·—, two-dimensional LSD wave model; -----, unsteady spherical wave model.

Experimental Results and Comparison

Streak photographs have been taken to show the spatial development of the plasma. Two plasma fronts are seen to develop axially with a supersonic velocity: 1) a first front expands toward the laser due to the absorption of a part of the laser energy, 2) another part of energy, transmitted through the absorbing front, supports a second front which propagates in the same direction of the beam.

In Fig. 6, the experimental data pointed out by solid circles have been obtained for an average intensity of about 2×10^7 W/cm^2 (peak intensity near the breakdown threshold). The solid line represents the results of the unsteady spherical calculations. For this intensity, we can observe that the plasma has a nearly spherical expansion, implying that the absorption of the energy is weak in the first luminous front. Air plasma is observed to grow as a volume absorbing plasma. In the case of a higher intensity, the character of the plasma expansion changes. The axial development is more important than the radial development (Fig. 5b).

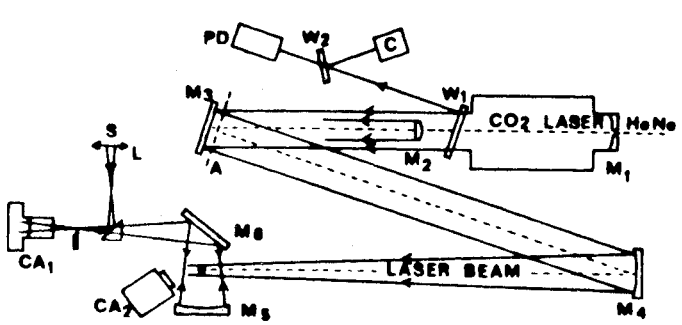

Fig. 4 Experimental setup. A = attenuators; C = calorimeter; CA_1,CA_2 = camera; L = convergent lens M_1 to M_6 plane or concave mirrors; PD = photon-drag detector; S = light source; W_1W_2 = Nacl windows; He-Ne alignment.

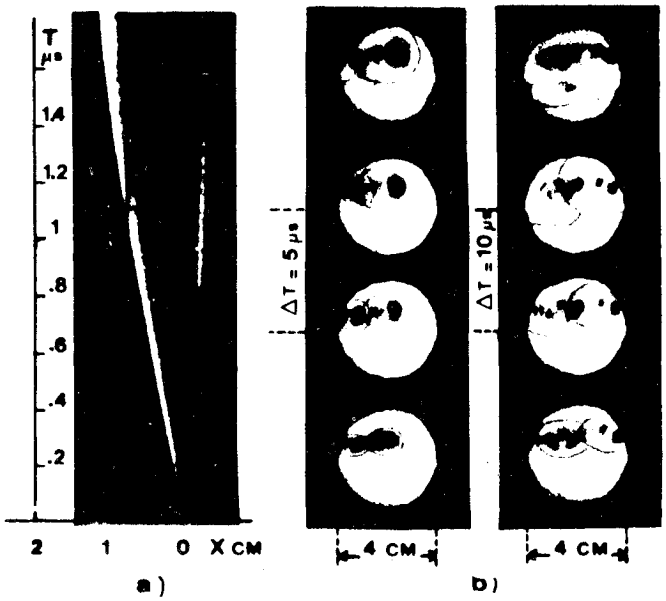

Fig. 5 High-speed photographs of aerosol-induced air breakdown. a) Streak photograph of the axial plasma expansion, T_c = time of breakdown. In this case, the laser beam is incident from the left. $\bar{\phi} = 10^8$ W/cm^2. b.) Schlieren photographs of the shock waves. The laser is incident from the right. $\bar{\phi} = 7 \times 10^7$ W/cm^2 ($\phi_{peak} \simeq 3.5 \times 10^8$ W/cm^2).

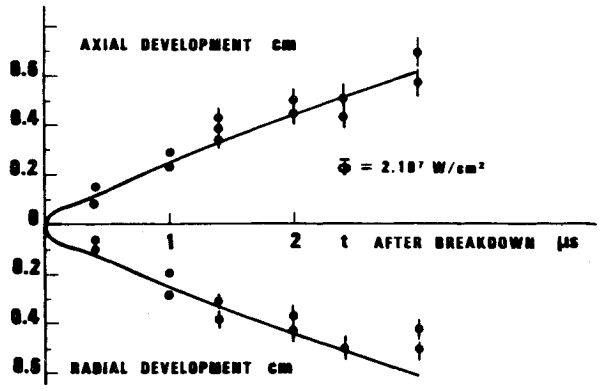

Fig. 6 Axial and radial developments of the shock wave. $\phi = 2 \times 10^7$ W/cm^2; —, calculated results; •, experimental data.

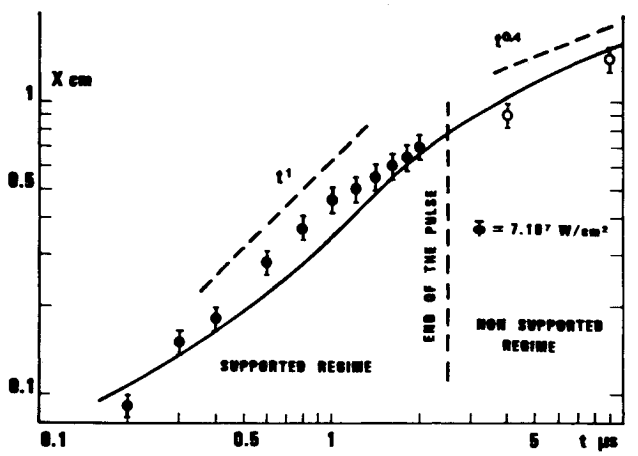

Fig. 7 Axial development as a function of time compared with calculated results (—); $\bar{\phi} = 7 \times 10^7$ W/cm^2 (•, ○) measurements deduced from streak and schlieren records, respectively. In the supported regime $X(t) \propto t^1$; in the nonsupported regime $X(t) \propto t^{0.4}$.

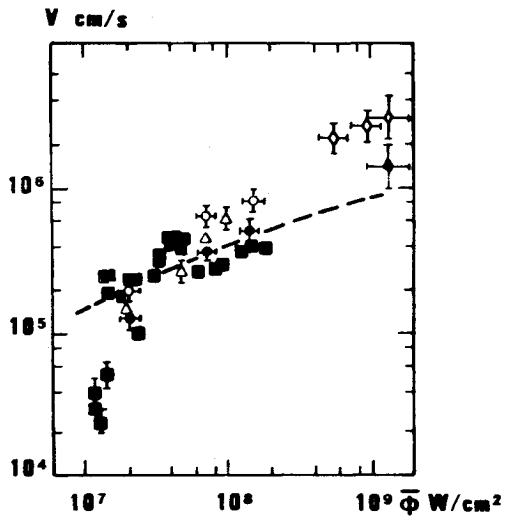

Fig. 8 Expansion velocity of the shock wave observed in different aerosol-induced breakdown experiments as a function of the laser intensity. ○ axial velocity; • radial velocity (Lencioni and Pettingill,[6,7] CO_2 laser); ■ mean velocity (Schlier et al.,[18] CO_2 laser); ◇ axial velocity, ◆ radial velocity (Amimoto et al.,[11] DF laser); △ axial velocity (Autric et al., CO_2 laser); and --- numerical results.

Logarithmic representation of time-dependent axial development for an average intensity of about 7×10^7 W/cm^2 (peak intensity 3.5×10^8 W/cm^2) is presented in Fig. 7. The solid circles represent experimental data obtained by means of the streak photographs, and the open circles represent results obtained by means of the schlieren photographs. The numerical results have been plotted with a solid line.

The logarithmic presentation shows two different regimes of the shock wave expansion. The first stage corresponds to a regime of supported laser-driven shock waves. One can notice that, after 0.5 μs, the expansion becomes quasistationary, corresponding to a laser-supported detonation expansion ($M \simeq 10$). In the second stage, the supported regime gives way to a spherical blastwave expansion ($M \simeq 3$) which can be related to the similar solution for a punctual explosion ($X \propto t^{0.4}$). In Figs. 6 and 7, numerical results of the shock wave development as a function of time for laser average intensities 2×10^7 and 7×10^7 W/cm^2 compare favorably with experimental results.

Figure 8 shows a compilation of experimental data obtained by several authors[6,7,9,11,18] for various experimental conditions. The velocities of development obtained in the steady-state region are plotted as a function of average laser intensity. The numerical results are shown by the dashed line.

In the low-intensity regime ($< 3 \times 10^7$ W/cm^2), the experimental data are lower than results of our model because the model does not take into account the effect of electron diffusion and energy loss mechanisms that decrease the plasma absorption coefficient. For this range of intensity, Wu's model is a better approximation to describe the plasma expansion. In the high-intensity regime ($> 3 \times 10^8$ W/cm^2) experimental data show an unsymmetrical expansion due to high absorption of the laser energy in an absorbing front which propagates toward the laser. Finally, calculations deduced from the present model are valid over an intensity range extending from about 3×10^7 to 3×10^8 W/cm^2.

Conclusion

The hydrodynamic model presented in this paper, of the development of a supported laser-driven shock wave, has showed a good agreement with the existing experimental data for high intensities ($> 3 \times 10^7$ W/cm^2). This model is actually used in a numerical code simulating the propagation of a high-energy pulsed CO_2 laser beam through the atmosphere.

Acknowledgment

The authors would like to thank J. P. Fragassi for his assistance throughout the course of the experiments.

References

[1] Canavan, G. H., Proctor, W. A., Nielsen, P. E., and Rockwood, S. D., "CO_2 Laser Air Breakdown Calculations," *Journal of Quantum Electronics*, Vol. QE8, 1972, p. 564.

[2] Kroll, N. and Watson, K. M., "Theoretical Studies of Ionization of Air by Intense Laser Pulses," *Physical Review*, Vol. A5, April 1972, pp. 1833-1905.

[3] Marquet, L. C., Hull, R. J., and Lencioni, D. E., Studies in Breakdown in Air Induced by a Pulsed CO_2 Laser," *Journal of Quantum Electronics*, Vol. QE8, 1972, p. 564.

[4] Lencioni, D. E., "The Effect of Dust in 10.6 μm Laser Induced Air Breakdown," *Applied Physics Letters*, Vol. 23, July 1973, pp. 12-14.

[5] Smith, D. C. and Brown, R. T., "Aerosol-Induced Air Breakdown with CO_2 Laser Radiation," *Journal of Applied Physics*, Vol. 46, March 1975, pp. 1146-1154.

[6] Lencioni, D. E., "The Limitations Imposed by Atmosphere Breakdown on the Propagation of High Power Laser Beams," *AGARD Conference Proceedings*, No. 183, Oct. 1975, pp. 32.1-32.12.

[7] Lencioni, D. E. and Pettingill, L. C., "The Dynamics of Air Breakdown Initiated by a Particle in a Laser Beam," *Journal of Applied Physics*, Vol. 48, May 1977, pp. 1848-1851.

[8] Smith, D. C., "Gas Breakdown Initiated by Laser Radiation Interaction with Aerosols and Solid Surfaces," *Journal of Applied Physics*, Vol. 48, June 1977, pp. 2217-2225.

[9] Reilly, J. P., Singh, P., and Weyl, G., "Multiple Pulse Laser Propagation Through Atmosphere Dusts at 10.6 Microns," AIAA Paper 77-697, June 1977.

[10] Autric, M., Caressa, J. P., Bournot, Ph., Dufresne, D., and Sarazin, D., "Propagation of Pulsed Laser Energy Through the Atmosphere," *AIAA Journal*, Vol. 19, Nov. 1981, pp. 1415-1421.

[11] Amimoto, S. T. et al., "Pulsed DF Chain-Laser Breakdown Induced by Maritime Aerosols," AIAA Paper 82-0894, June 1982.

[12] Vigliano, P., Autric, M., Caressa, J. P., Chhim, V., and Inglésakis, G., "Hydrodynamical Models of Aerosol-Induced Breakdown," Paper 24, 4th International Symposium on Gas Flow and Chemical Lasers, Stresa, Italy, Sept. 1982.

[13] Raizer, Yu. P., "Heating of a Gas by Powerful Light Pulse," *Soviet Physics JETP*, Vol. 21, Nov. 1965, pp. 1009-1017.

[14] Edwards, A. L. and Fleck, J. A. Jr., "Two-Dimensional Modeling of Aerosol-Induced Breakdown in Air," *Journal of Applied Physics*, Vol. 50, June 1979, pp. 4308-4313.

[15] Boni, A. A. and Su, F. Y., "An Analytical Technique for Laser-Driven Shock Waves," *Acta Astronautica*, Vol. 1, 1974, pp. 761-780.

[16] Bach, G. G. and Lee, J. H. S., "An Analytical Solution for Blast Waves," *AIAA Journal*, Vol. 8, 1970, pp. 271-275.

[17] Spitzer, L., "Physique des gaz completement ionisés," Dunod, Paris, 1959.

[18] Schlier, R. E., Pirri, A. N., and Reilly, D. J., "Air Breakdown Studies," AFWL-TR 72-74, Feb. 1973.

[19] Wu, P. K. and Pirri, A. N., "The Dynamics of Air Plasma Growth in a 10.6 μm Laser Beam," AIAA Paper 78-176, Jan. 1978.